ANTIMICROBIAL AGENTS AND CHEMOTHERAPY, Feb. 2005, p. 749–759 Vol. 49, No. 2
0066-4804/05/$08.00+0 doi:10.1128/AAC.49.2.749–759.2005

Discovering the Mechanism of Action of Novel Antibacterial Agents through Transcriptional Profiling of Conditional Mutants

C. Freiberg,[1] H. P. Fischer,[2] and N. A. Brunner[1]*

Bayer HealthCare AG, Pharma Research, Wuppertal, Germany,[1] and Genedata, Basel, Switzerland[2]

Received 4 June 2004/Returned for modification 16 August 2004/Accepted 3 October 2004

We present a new strategy for predicting novel antibiotic mechanisms of action based on the analysis of whole-genome microarray data. We first built up a reference compendium of *Bacillus subtilis* expression profiles induced by 14 different antibiotics. This data set was expanded by adding expression profiles from mutants that showed downregulation of genes coding for proven or emerging antibacterial targets. Here, we investigate conditional mutants underexpressing *ileS*, *pheST*, *fabF*, and *accDA*, each of which is essential for growth. Our proof-of-principle analyses reveal that conditional mutants can be used to mimic chemical inhibition of the corresponding gene products. Moreover, we show that a statistical data analysis combined with thorough pathway and regulon analysis can pinpoint the molecular target of uncharacterized antibiotics. We apply this approach to two novel antibiotics: a recently published phenyl-thiazolylurea derivative and the natural product moiramide B. Our results support recent findings suggesting that the phenyl-thiazolylurea derivative is a novel phenylalanyl-tRNA synthetase inhibitor. Finally, we propose a completely novel antibiotic mechanism of action for moiramide B based on inhibition of the bacterial acetyl coenzyme A carboxylase.

Infectious diseases remain a serious threat to public health. Rapid resistance development among major pathogens makes antibiotics more and more ineffective, raising the need to find novel structural classes of antibiotics (7). A critical bottleneck in the development of novel classes of antibacterial agents is the limited understanding of the molecular mechanism of action (MOA) of bioactive substances. Genome-wide expression technologies together with advanced data analysis techniques are now widely used to elucidate the bacterial defense mechanisms against antibiotic stress (11, 20, 38). The mRNA profiles triggered in response to antibiotic stress were shown to represent characteristic signatures of the specific stress type and reflect the specific transcriptional response of the cell to the inhibition of certain physiological functions. For instance, treatments with DNA gyrase inhibitors have been reported to predominantly induce DNA repair enzymes (19, 56). Agents blocking mycolic acid biosynthesis have been shown to change the expression of corresponding biosynthetic enzymes in *Mycobacterium tuberculosis* (4, 63). Compounds interfering with protein biosynthesis induce genes coding for ribosomal proteins or other MOA-specific gene groups (43, 51).

However, as antibiotics are supposed to inhibit bacterial growth, they also change the expression of a wide range of genes not directly linked to the target's function, which in many cases obscures the primary antibiotic effect. Therefore, in order to deduce characteristic signatures for antibiotics, comparative global expression analyses need to be performed on the basis of a large collection of diverse mRNA profiles that represent different cellular stress states. A so-called reference compendium of expression profiles makes it possible to classify the MOA of antibiotics and to pinpoint the typically very few compound- or MOA-specific marker genes. Recently, Hutter et al. (30) used a reference compendium based on the gram-positive model bacterium *Bacillus subtilis* to classify the MOAs of antibacterial compounds by using support vector machine algorithms. Complementary to this work, Fischer et al. (16) proposed an integrated genome expression data analysis strategy to identify and characterize antibiotic-responsive regulatory networks.

The present mRNA reference compendium approaches to antibiotic MOA characterization suffer from the limitation that only mechanisms that are employed by already existing antibiotics can be predicted. The expansion of a reference compendium with expression profiles of bacterial mutants underexpressing potential target proteins could therefore be a helpful means to overcome this hurdle in identifying novel antibacterial MOAs. In this study, we generated a compendium of genome-wide expression profiles, representing the response of *B. subtilis* to treatment with 14 chemically diverse antibiotics. The data representing chemically induced mRNA profiles were supplemented by conditional mutant profiles, representing the effect of underexpressing four distinct essential genes or operons encoding antibacterial target proteins. Here, we focus on the target areas of aminoacyl-tRNA synthesis (AATS) and fatty acid biosynthesis (FAB). In mutant ILES(−) and mutant FABF(−), genes were downregulated which encode two classical antibacterial targets: the isoleucyl-tRNA synthetase and the type II β-ketoacyl-acyl carrier protein synthetase. Similarly, in mutants PHEST(−) and ACCDA(−) the amounts of transcripts were reduced; these transcripts code for two emerging targets: the phenylalanyl-tRNA synthetase (PheST) and the carboxyltransferase subunits (AccDA) of the acetyl coenzyme A (acetyl-CoA) carboxylase (ACC).

First, we show that downregulation of target genes causes transcriptional responses similar to those generated by respective antibiotic treatments as demonstrated with the well-investigated cerulenin (known to target FabF in *B. subtilis*) and mupirocin (known to inhibit IleS) (29, 34, 40). Second, we

* Corresponding author. Mailing address: Bayer HealthCare AG, Pharma Research, 42096 Wuppertal, Germany. Phone: 49 202 365206. Fax: 49 202 364116. E-mail: nina.brunner@bayerhealthcare.com.

TABLE 1. Oligonucleotides used in this study

Oligonucleotide	Sequence
5′-End amplification of the *B. subtilis* genes *fabF, ileS,* and *pheS*	
FABF1	5′-ATCGGATCCGCAATCCGCTGGGGCCG-3′
FABF2	5′-ATCGGATCCGCACGAAAAACGGGCTTACC-3′
ILES1	5′-ATCGGATCCATGGATTTTAAAGACACGCTC-3′
ILES2	5′-ATCGGATCCGTCACCGCGGACACCAAG-3′
PHES10	5′-ATCGGATCCGGTTTGTTTACATAAAAGGAGG-3′
PHES20	5′-ATCGGATCCGCCGCCGACTGCAACAGG-3′
Amplification of the operon *accDA* from *B. subtilis*	
ACCADR	5′-ATCGGATCCATGTTAAAGGATATATTCACGAAAAAG-3′
ACCADT	5′-ATCGGATCCTTAGTTTACCCCGATATATTGATC-3′
Amplification of the neighboring regions of *accDA* from *B. subtilis*	
ACCAD1A	5′-ATCGGATCCTTGAAGCCATTGCTTCACTGG-3′
ACCAD1B	5′-TGCGGCCGCTAAATCTAGACTCGTGAATATATCCTTTAACAAATG-3′[a]
ACCAD2A	5′-AGTCTAGATTTAGCGGCCGCATATATCGGGGTAAACTAAATAAACG-3′[a]
ACCAD2B	5′-ATCGGATCCGAATGTCATTATCAATTGTACCCG-3′
Pairs used in qRT-PCR for measurement of different *B. subtilis* transcripts (*accA, fabF, pheS, pheT, ileS, fabHB, yurP,* and 16S rRNA)	
ACCA1	5′-AAAAGCGCTTCGTCTGATGA-3′
ACCA2	5′-CGCTCCGCCTTTTACTTCTT-3′
FABF3	5′-TGTCGGCTACGGCTCAACC-3′
FABF4	5′-GCGGGCTTCATCAGGCACATAA-3′
PHES30	5′-GCGCGATATGCAGGACAGC-3′
PHES40	5′-CCGGCACCGAGGATTTCAA-3′
PHET1	5′-GGGCAGAACAGCGAACATTTTATT-3′
PHET2	5′-GCGCCTTTGTCACTTCTTCTTCAG-3′
ILES3	5′-ATCGGATCCATGGATTTTAAAGACACGCTC-3′
ILES4	5′-GCCTCGTTTTGCCATTTCAC-3′
FABHB1	5′-GCCGGGATTTCTTGCGTCTGTA-3′
FABHB2	5′-GCTTCCCGGCTTTCACTGC-3′
YURP1	5′-CAGTACGATTGGGGTGATGAGG-3′
YURP2	5′-TCTAAACCGAGCAGGATGATAAAC-3′
RRNA16S1	5′-CGTGGGGAGCGAACAGGATTAGAT-3′
RRNA16S2	5′-TTGTCACCGGCAGTCACCTTAGAG-3′

[a] The complementary tag sequence for PCR product assembling is underlined.

demonstrate that a reference compendium including underexpression mutant profiles enables automated MOA classification, by using mRNA profile classification algorithms. Third, we show that prediction of the molecular target of novel antibacterials is possible with such a combined chemical and mutant data compendium. By applying our analysis strategy, we are able to independently support the recently published PheST inhibition mechanism of a novel phenyl-thiazolylurea (PTU) derivative (5). Finally, we find that one of our mutant profiles matches the mRNA profile induced by the natural product moiramide B (MOIB) (42). Based on our MOA analysis techniques, the mRNA profiles triggered by this compound suggest that the antibiotic activity of MOIB is most likely due to inhibition of ACC, representing a completely novel antibacterial mechanism.

Our MOA analysis strategy consists of three major levels. First, we automatically classify compounds and underexpression effects based on a reference compendium of expression profiles, using an algorithm based on a nonparametric statistical test. Second, we analyze the expression patterns of major regulons and biosynthetic pathways by investigating the statistical overrepresentation of key pathways. Third, we focus on the detailed expression activity of individual pathways to identify the actual molecular target of the compounds under investigation.

MATERIALS AND METHODS

Construction of conditional *B. subtilis* mutants. Construction of plasmids for *B. subtilis* transformation was performed in *Escherichia coli* XL1-Blue (Stratagene, La Jolla, Calif.). Genetic techniques with *B. subtilis* including transformation procedures were applied as described previously (26).

Four genes or operons (*ileS*, *fabF*, *pheST*, and *accDA*) were each put under the control of a xylose-inducible promoter, resulting in strains called *B. subtilis* ILES(−), FABF(−), PHEST(−), and ACCDA(−), respectively. The first three strains were generated as follows. The 5′ ends of the genes were amplified from genomic *B. subtilis* DNA (Table 1) and cloned into the vector pJH101 (15) via the BamHI restriction site. *B. subtilis* was transformed with the resulting constructs and selected on Luria-Bertani (LB) medium with 0.25% (wt/vol) xylose and 3 μg of chloramphenicol/ml, the marker for pJH101 integration (single recombination). While the genes of interest were all located downstream of the xylose-dependent promoter, 5′ fragments of the respective genes remained under the control of the wild-type promoters.

B. subtilis ACCDA(−) was generated by ectopic expression of the operon *accDA* under the control of the xylose-inducible promoter P_{xylA}. This was achieved by amplification of the *accDA* operon with the primers ACCADR and ACCADT (Table 1), followed by subcloning into the expression vector pDG1731xyl (24) via the BamHI site and subsequent integration at the *thrC* locus

TABLE 2. Compounds and their concentrations used for transcriptome analysis

Compound name	Abbreviation	MIC (μg/ml)	Applied concn (fold MIC)
Actinonin	ACT	16.00	2.00
Azaserine	AZA	2.00	0.50
Azithromycin	AZI	1.00	2.00
Phenyl-thiazolylurea derivative	PTU	8.00	0.03
Cerulenin	CER	16.00	2.00
Gentamicin	GEN	0.13	2.00
Chloramphenicol	CHL	4.00	1.00
Ciprofloxacin	CIP	0.25	4.00
Methicillin	MET	0.13	2.00
Moiramide B	MOIB	4.00	2.00
Mupirocin	MUP	0.06	1.00
Nalidixic acid	NAL	16.00	1.00
Oxacillin	OXA	0.50	1.00
Vancomycin	VAN	0.25	2.00

of the *B. subtilis* chromosome by marker exchange as described previously (22). The wild-type locus of *accDA* was deleted in the resulting strain *B. subtilis* MH41 as follows. The neighboring regions of *accDA* were amplified by PCR with the oligonucleotides ACCAD1A and ACCAD1B for amplification of the upstream region as well as ACCAD2A and ACCAD2B for amplification of the downstream region (Table 1). The primers were designed such that the ends of the PCR products facing the 5′ and 3′ regions of the genes carried a complementary tag sequence (Table 1). This tag sequence was used to assemble the products in a second PCR with the outward primers. The outward primers contained terminal BamHI restriction sites allowing cloning of the fusion PCR product into the BamHI site of pJH101. The sequence cloned into pJH101 internally contained the tag sequence with XbaI and NotI sites for cloning of a neomycin resistance cassette derived from pBEST501 (33). The resulting pJH101 derivative was transformed into *B. subtilis* MH41, and selection for deletion by double recombination was performed as described previously (24).

Growth experiments and RNA isolation. Cultures of *B. subtilis* 168 were grown in Belitzky minimal medium (58) to an optical density at 600 nm (OD_{600}) of 0.4 at 37°C. After removal of an aliquot (time zero, untreated sample), the remaining culture was subjected to compound stress by addition of antibiotics (Table 2) and incubated for a further 10 and 40 min to obtain aliquots of treated cells (time points 1 and 2, respectively). Empirically, we found that the applied compound concentrations should be as high as possible but should not cause more than 25% growth reduction compared to the control at time point 2. Cell harvesting and RNA isolation were performed as described recently (16).

The conditional *B. subtilis* mutants were grown overnight at 37°C in Belitzky minimal medium with 0.25% xylose and 3 μg of chloramphenicol/ml [or without antibiotic in the case of strain ACCDA(−)] after inoculation with colonies from LB agar plates with the same supplements. In order to deplete xylose and consequently to reduce the expression level of the target genes (underexpression), the cells were centrifuged, washed twice in phosphate-buffered saline (20 mM potassium phosphate, 150 mM NaCl), and inoculated in 200 ml of prewarmed Belitzky minimal medium with 3 μg of chloramphenicol/ml [or without antibiotic in the case of ACCDA(−); start OD_{600} = 0.05]. After having reached the OD_{600} of approximately 0.2 at 37°C, the cells were transferred into fresh medium with an OD_{600} of 0.05 for further incubation. When necessary, the procedure was repeated once more, so that the mutant growth rate was reduced by more than 80% in comparison to the *B. subtilis* 168 wild type, which was treated in the same way. The mutants as well as wild-type cells were harvested for RNA isolation at an OD_{600} of approximately 0.2 as described above. The 80% growth reduction criterion was chosen after preexperiments with faster-growing mutants, for which the transcriptome data revealed too few deregulated genes (data not shown).

cDNA labeling and microarray experiments. Generation of fluorescence-labeled cDNA, hybridization with *B. subtilis* whole-genome arrays (Eurogentec), and image analysis with the Axon GenePix 400A confocal laser scanner (Axon Instruments) were performed as described previously (16).

Expression data analysis. The quality of the expression profiling experiments was checked as outlined previously (16) by using the Expressionist 4.1 software (Genedata, Basel, Switzerland). The quality-checked signals of all features were used for a global microarray normalization, with the scaling factor being calculated with the requirement that the sum of all logarithmized values in the Cy3 channel equals the sum of all logarithmized values in the Cy5 channel. For each condition, duplicates or triplicates of microarray experiments were performed, whereas for each gene the average fold factor was calculated on the basis of logarithms of the signal ratios.

For an estimate of the inherent biological variability of our *B. subtilis* cultures, we treated three independently grown *B. subtilis* cultures with cerulenin (16). We then calculated for this representative experiment set the standard deviation of the fold factor as 0.164. This means that a fold factor of 1.4 (or 1/1.4) already represents 3 standard deviations of the Gaussian distribution function (equivalent to a *P* value of >99.73%).

Automated MOA classification. The averaged expression fold factors for the 40-min compound exposure experiments together with the mutant data were used for MOA classification. The a priori assignments of the reference compounds and underexpression effects to categorical MOA classes were performed according to the literature and present biological knowledge (see Results). A consistency check of the precategorized compound-mRNA profiles was performed (cross-validation) by removing individual compound profiles or pairs of compound- and mutant-based profiles (see Results) one after another from the reference set and reclassifying the profile(s) based on the remaining (N-1 or N-2) reference profiles.

Cross-validation as well as classification of novel profiles was performed using the Wilcoxon classifier implemented in Expressionist (Genedata). In brief, this statistical method needs a "query expression profile" as input (e.g., representing an expression profile triggered by a novel compound). In a first step, correlation coefficients of this profile are calculated with regard to all reference experiments in the reference compendium database. Ranking the reference experiments by their corresponding correlation coefficients leads to a sorted list reflecting their global similarity to the query gene expression profile. In an ideal case, one would expect that all the top experiments belong to one MOA class, with the other MOA classes being distributed in the lower parts of the rank list. In order to define a quantitative measure for the rank separation of the gene expression correlations and their associated a priori MOA classes, a Wilcoxon test was employed. Here, the Wilcoxon test was used to check for the separation of two classes, which are the correlation coefficients belonging to a given MOA class compared to the correlations of all other MOA classes. A one-sided Wilcoxon test probes how well these two groups separate in terms of their ranking distribution. In this way, all MOA categories represented in our reference compendium were investigated. Applying a one-sided Wilcoxon test enables us to calculate *P* values for all query experiments and all represented MOAs. The so-called "affinity values" (*A*) are then calculated as the inverse error function of the Wilcoxon test's *P* value, $A = \mathrm{erf}^{-1}(p_{\mathrm{Wilcoxon}})$, reflecting the MOA assignment affinity.

Gene expression correlation analyses and promoter prediction. Correlation analyses based on gene expression data were performed using Expressionist 4.1 (Genedata). Operon and promoter prediction was performed using Phylosopher 4.0 (Genedata). The algorithms have been described previously (16).

Differential MIC determination. Microdilution MICs were determined against *B. subtilis* strains in 96-well microtiter plates in LB medium containing a 0 or 0.25% xylose concentration and serial dilutions (twofold) of antibiotics. The precultures of the conditional mutants ILES(−), FABF(−), and PHEST(−) additionally contained 3 μg of chloramphenicol/ml. Various starting inocula were used in the range of 10^4 to 10^6 CFU ml^{-1} derived from precultures grown for 3 h in LB medium with 0 or 0.25% (wt/vol) xylose. The MIC was the lowest concentration of drug that yielded no visible growth after incubation for 18 to 24 h at 37°C. Endpoints were determined by measuring the OD_{600} with the microtiter plate reader EL312e (Bio-Tec Instruments).

qRT-PCR. For selected genes, measurements of relative transcript amounts were performed by quantitative reverse transcription-PCR (qRT-PCR) with the QuantiTect SYBR Green RT-PCR kit (Qiagen) according to the manufacturer's instructions. The same RNA samples were used for cDNA synthesis and subsequent quantitative PCR as for microarray experiments. Specific primer pairs were selected for the genes *accA*, *fabF*, *pheS*, *pheT*, *ileS*, *fabHB*, and *yurP* (Table 1). In addition, a piece of the 16S rRNA was quantified, in order to normalize the obtained expression values of selected genes to the amount of 16S rRNA in each RNA sample (Table 1). The reactions were performed on an ABI Prism 7700 Sequence Detection system (PE Applied Biosystems), during which the fluorescence signal from SYBR Green intercalation was monitored to quantify the double-stranded DNA product formed after each PCR cycle. The difference (*n* = fold) in the initial concentration of each transcript (normalized to 16S rRNA) with respect to the wild type was calculated according to the comparative Ct method according to the equation $2^{-\Delta\Delta Ct}$ (ABI user bulletin).

TABLE 3. Relative expression levels of genes in conditional mutants

B. subtilis strain	Avg growth rate reduction (%)	Xylose-dependent gene-operon	Relative expression of xylose-dependent gene (qRT-PCR)	Selected gene for confirmation of microarray data	Relative expression value (qRT-PCR)	Relative expression value (microarray)
ILES(−)	91	*ileS*	0.32 ± 0.04	*yurP*	13.55 ± 2.26	6.35 ± 1.34
FABF(−)	92	*fabF*	0.10 ± 0.03	*fabHB*	14.76 ± 0.70	12.63 ± 2.03
PHEST(−)	90	*pheST*	0.02 ± 0.00	*yurP*	58.08 ± 9.71	45.53 ± 3.63
ACCDA(−)	83	*accDA*	0.14 ± 0.05	*fabHB*	0.19 ± 0.04	0.43 ± 0.03

RESULTS

Global mRNA expression profiling for MOA analyses. The influence of antibiotics on the transcriptome of logarithmically growing *B. subtilis* cells was measured using fluorescent DNA microarray technology. The bacterial cultures were treated with each compound for 10 and 40 min (time points 1 and 2, respectively). The applied compound concentrations are listed in Table 2. The reference compendium for automated MOA classification was compiled from the 40-min experiments, while the 10-min data were additionally used to study the primary effects of antibiotics on the transcriptome by pathway analyses (see below). In addition, four *B. subtilis* mutants were generated during this study, in which essential genes or operons were each put under the control of a xylose-inducible promoter. The mutants were depleted of xylose and consequently reduced in their growth rate. Clear reduction (>80%) of growth rate was necessary to see significant effects on the transcriptome level. The averaged expression values for each compound and mutant can be found online at http://www.genedata.com/publications/supplements/. The relative expression values of the genes downregulated in the mutants were determined by qRT-PCR, since the full-length gene probes on the chip were not suitable for discriminating between the conditionally expressed transcripts and respective inactive fragments expressed from the wild-type promoter (Table 3). Two genes, *yurP* and *fabHB*, were also quantified by qRT-PCR, in order to confirm the microarray data (Table 3).

Automated MOA prediction by applying mRNA profile classification algorithms: antibiotics versus mutant patterns. Based on the expression profiles, we built a reference classification system, reflecting the MOAs of 13 antibiotics (12). The topoisomerase II-IV-targeting quinolones nalidixic acid and ciprofloxacin as well as the purine nucleotide synthesis inhibitor and DNA carboxymethylating agent azaserine (36, 37) were grouped into the DNA synthesis inhibitor class (DNA). The ribosome-targeting antibiotics gentamicin, azithromycin, and chloramphenicol as well as the peptide deformylase inhibitor actinonin were classified as protein biosynthesis inhibitors (protein). The glycopeptide vancomycin and the beta-lactams methicillin and oxacillin represent cell wall biosynthesis inhibitors (cell wall). The FabF inhibitor cerulenin and the IleS inhibitor mupirocin as well as the recently published PheST inhibitor PTU were combined into one class of fatty acid biosynthesis and aminoacyl-tRNA synthetase inhibitors (FAB-AATS) because of high similarities of their expression profiles (see the next section). In addition to the chemically induced profiles, the FAB-AATS class was supplemented with mRNA profiles of the conditional mutants FABF(−), ILES(−), and PHEST(−), mutants that were shown to exhibit differential sensitivity to the respective antibiotics (Table 4).

To make use of these profiles for automated MOA prediction, we used a Wilcoxon classifier, as implemented in the Expressionist system (Genedata). This classification algorithm enables the categorization of a given mRNA profile to an antibiotic MOA class (see Materials and Methods). The reference compendium data were checked for internal consistency by using the a priori MOA assignments. For this a cross-validation procedure was applied, in which the averaged profile of each compound was consecutively removed from the reference set (the so-called "leave-one-out" strategy) and reclassified on the basis of the remaining (N-1) reference profiles, as if the compound's a priori MOA assignment would have been unknown. By using the mRNA profiles of 13 chemically induced and three mutant expression profiles, all MOAs were correctly assigned (Table 5). This result shows that the data set at hand is consistent with regard to the predefined MOA assignments and that the Wilcoxon classifier algorithm is indeed able to distinguish the various profiles representing the different broad MOA classes. Secondly, these findings demonstrate that the mRNA profiles of the FABF(−), ILES(−), and PHEST(−) mutant profiles fall into the same MOA categories as their chemically induced counterparts (Table 5). Thirdly, the expression profiles of the antibiotic PTU as well as the profiles of the PHEST(−) mutant were classified into the FAB-AATS category. As recently published, PTU represents a novel PheST inhibitor, which was derived from a hit identified in an enzymatic high-throughput screening of large compound libraries (5).

To characterize the MOA of the natural product MOIB, a compound with an unknown MOA, we used again the Wilcoxon classifier. MOIB was assigned to the FAB-AATS class on the basis of the reference compendium. A more detailed

TABLE 4. Differential sensitivity of conditional mutants derived from *B. subtilis* 168

Strain	Inoculum, (CFU/ml)	MIC (μg/ml) of compound[a] with (+) or without (−) xylose									
		MUP		CER		PTU		MOIB		CIP	
		+	−	+	−	+	−	+	−	+	−
168	1.0×10^5	0.08	0.08	20	20	12	12	1	1	0.08	0.08
ILES(−)	1.0×10^6	0.04	0.005							0.16	0.08
FABF(−)	1.0×10^5			5	0.04					0.06	0.06
PHEST(−)	1.0×10^5					12	0.2			0.08	0.08
ACCDA(−)	2.5×10^4							1	0.1	0.04	0.04

[a] MUP, mupirocin; CER, cerulenin; PTU, phenyl-thiazolylurea derivative; MOIB, moiramide B; CIP, ciprofloxacin.

TABLE 5. MOA classification of antibiotics and underexpression effects in conditional mutants based on whole-genome expression profiles[a]

Compound or mutant[b]	Predefined MOA class	MOA classifier affinity value				MOA assignment
		DNA	Protein	Cell wall	AATS-FAB	
AZA	DNA	**1.561**	−1.569	0.1021	0.25	DNA
NAL	DNA	**1.441**	−1.292	−0.6124	0.6667	DNA
CIP	DNA	**1.321**	−0.3693	0.1021	−0.6667	DNA
ACT	Protein	0.5103	**1.837**	0.4082	−2.25	Protein
GEN	Protein	0.1021	**1.837**	0.8165	−2.25	Protein
CHL	Protein	−0.3062	**1.837**	−0.1021	−1.167	Protein
AZI	Protein	0.5103	**1.837**	0.2041	−2.083	Protein
OXA	Cell wall	0.2041	−1.477	**1.561**	0.08333	Cell wall
MET	Cell wall	−0.9186	−1.108	**1.561**	0.6667	Cell wall
VAN	Cell wall	−1.021	−1.477	**1.321**	1.25	Cell wall
CER	AATS-FAB	0.2752	−1.9	0.8257	**0.9**	AATS-FAB
FABF(−)	AATS-FAB	−0.6055	−1.7	0.2752	**2**	AATS-FAB
MUP	AATS-FAB	−0.3853	−2	0.3853	**2**	AATS-FAB
ILES(−)	AATS-FAB	−0.3853	−2	0.4954	**1.9**	AATS-FAB
PTU	AATS-FAB	−0.1651	−2	0.3853	**1.8**	AATS-FAB
PHEST(−)	AATS-FAB	0.05505	−1.9	0.05505	**1.8**	AATS-FAB
MOIB	?	−0.80861	−1.97	0.42809	**2.07**	AATS-FAB
ACCDA(−)	?	−0.61835	−1.2	0.1427	**1.46**	AATS-FAB

[a] Thirteen compounds and three mutants were preassigned to MOA classes based on a priori biological knowledge. Five global MOA classes were differentiated: DNA, DNA synthesis; Protein, protein synthesis; Cell wall, cell wall biosynthesis; and FAB-AATS, aminoacyl-tRNA synthesis–fatty acid biosynthesis. This compound MOA preassignment was cross-validated by taking out the profiles for each compound or compound-mutant pair (leave-one-out strategy) and subsequently reclassifying their profile(s) based on the remaining N-1 (N-2) compound profiles (see Materials and Methods). The affinity values represent the output of the Wilcoxon MOA classifier (Expressionist; Genedata). The compounds and mutants were automatically assigned to the MOA class for which the highest affinity value was calculated (boldface). The predicted MOA assignments are summarized. The results show an overall consistent picture, meaning that the reference compendium data are consistent with regard to the microarray data quality and the a priori MOA classification. For instance, the recently characterized PheST inhibitor PTU was indeed correctly assigned to the FAB-AATS class. Of particular importance is that the conditional mutants are correctly classified in their respective target classes. The results also indicate that the so-far-uncharacterized compound MOIB is acting via a previously unknown MOA. It is classified into the same FAB-AATS category as the mutant ACCDA(−) on the basis of the cross-validated reference compendium (last two rows).

[b] See Table 2 for definitions of drug abbreviations.

analysis of the transcriptionally activated regulons and pathways indicated that the ACC might be the target of this compound (see below). This finding suggested the generation of an appropriate conditional target mutant, ACCDA(−). This mutant indeed exhibited differential sensitivity to MOIB (Table 4), and its profile was also correctly categorized by the Wilcoxon classifier into the FAB-AATS category (Table 5), consistent with the classification of MOIB.

Antibiotic-induced regulon and pathway activation pattern analysis. The transcriptome data used for MOA classification were analyzed with a focus on the deregulation of major regulons and biosynthetic pathways. The genes representing 16 regulatory units and 12 (generalized) pathways or groups of pathways from *B. subtilis* were compiled based on the whole-genome annotation from Phylosopher (Genedata) and on the functional classifications derived from the COG database at the National Center for Biotechnology Information (60) (see http://www.genedata.com/publications/supplements/). Additionally, we compiled and incorporated information from selected publications. In this work, the following regulons were considered: *relA*-dependent stringent response (13); *fapR*-dependent FAB and phospholipid biosynthesis genes (16, 52); *lexA*-dependent SOS response (41); the *hrcA*- and *ctsR*-dependent class I and III heat shock regulons (53); and alternative RNA polymerase sigma factor-dependent regulons *sigB* (21, 46, 47), *sigD* (39), *sigH* (8), *sigF* (1, 14, 25, 45, 54), *sigE* (31, 32, 35, 45, 49, 59, 64), *sigG* (31, 45), *sigK* (18, 31, 44), *sigW* (10, 11, 48, 62), and *sigX* (9, 11, 28, 48). The not-yet-completely characterized *sigM* regulon (9, 11, 27, 61) was extended by additional candidate genes by a combined gene expression-genome sequence analysis. For this, we focused on the gene *ypuA*, a gene of unknown function that was among the genes most strongly induced by cell wall biosynthesis inhibitors. We ran correlation analyses against the whole reference compendium transcriptome data set. Prediction of operons composed of correlated genes, which are adjacent on the *B. subtilis* chromosome, was done using Phylosopher (Genedata). The 400-bp upstream regions of the 20 genes and operons, which represented the most highly correlated transcription units with regard to the *ypuA* profile, were searched for sigma factor binding sites similar to the one predicted upstream of *ypuA* (5′-TGAAAC-$N_{17–19}$-GTCT-3′), allowing for maximally two mismatches. Indeed, all top-20 genes and operons possess such binding sites, among these the sigma factor gene *sigM* itself as well as six additional genes and operons, for which *sigM*-dependent expression has been previously published (2) (see http://www.genedata.com/publications/supplements/).

In order to get a comprehensive overview of the induced and repressed regulons and pathways, we defined cutoff values for considering genes induced (expression values of ≥1.8) or repressed (expression values of ≤1/1.8). When at least 20% of genes belonging to a regulon or pathway were induced or repressed according to the definition mentioned above, the respective regulon or pathway was defined to be "deregulated." Figure 1A gives a comprehensive overview of the *B. subtilis* global response to a wide spectrum of antibiotics with different MOAs and a comparison of these effects to the corresponding mutant profiles. The detailed view of the pathway activation patterns revealed that FAB and AATS inhibition

A)

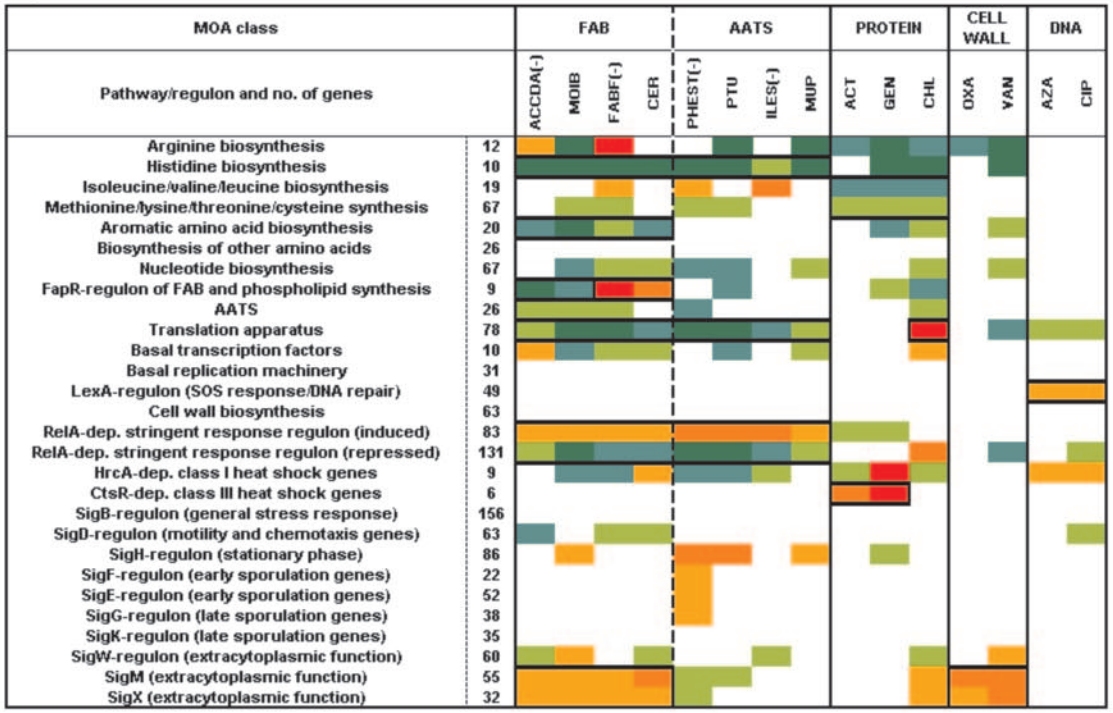
MOA class
FAB
AATS
PROTEIN
CELL WALL
DNA
Pathway/regulon and no. of genes
ACCDA(-)
MOIB
FABF(-)
CER
PHEST(-)
PTU
ILES(-)
MUP
ACT
GEN
CHL
OXA
YAN
AZA
CIP
Arginine biosynthesis 12
Histidine biosynthesis 10
Isoleucine/valine/leucine biosynthesis 19
Methionine/lysine/threonine/cysteine synthesis 67
Aromatic amino acid biosynthesis 20
Biosynthesis of other amino acids 26
Nucleotide biosynthesis 67
FapR-regulon of FAB and phospholipid synthesis 9
AATS 26
Translation apparatus 78
Basal transcription factors 10
Basal replication machinery 31
LexA-regulon (SOS response/DNA repair) 49
Cell wall biosynthesis 63
RelA-dep. stringent response regulon (induced) 83
RelA-dep. stringent response regulon (repressed) 131
HrcA-dep. class I heat shock genes 9
CtsR-dep. class III heat shock genes 6
SigB-regulon (general stress response) 156
SigD-regulon (motility and chemotaxis genes) 63
SigH-regulon (stationary phase) 86
SigF-regulon (early sporulation genes) 22
SigE-regulon (early sporulation genes) 52
SigG-regulon (late sporulation genes) 38
SigK-regulon (late sporulation genes) 35
SigW-regulon (extracytoplasmic function) 60
SigM (extracytoplasmic function) 55
SigX (extracytoplasmic function) 32

B)

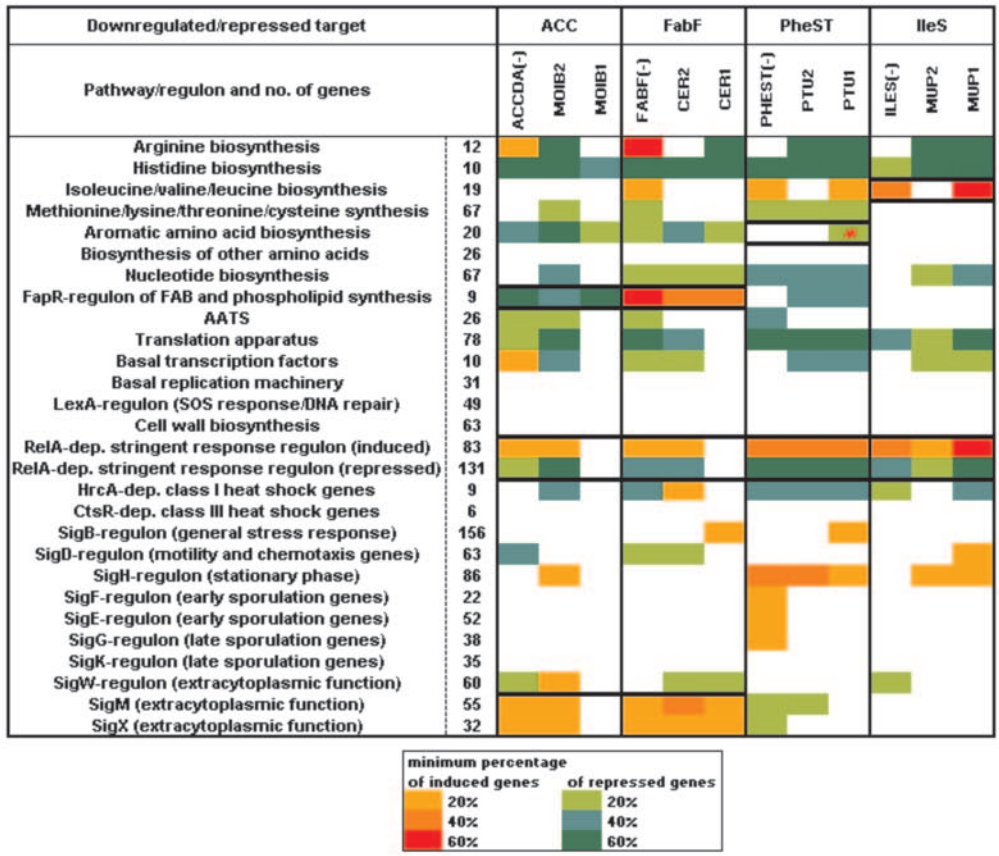
Downregulated/repressed target
ACC
FabF
PheST
IleS
Pathway/regulon and no. of genes
ACCDA(-)
MOIB2
MOIB1
FABF(-)
CER2
CER1
PHEST(-)
PTU2
PTU1
ILES(-)
MUP2
MUP1
Arginine biosynthesis 12
Histidine biosynthesis 10
Isoleucine/valine/leucine biosynthesis 19
Methionine/lysine/threonine/cysteine synthesis 67
Aromatic amino acid biosynthesis 20
Biosynthesis of other amino acids 26
Nucleotide biosynthesis 67
FapR-regulon of FAB and phospholipid synthesis 9
AATS 26
Translation apparatus 78
Basal transcription factors 10
Basal replication machinery 31
LexA-regulon (SOS response/DNA repair) 49
Cell wall biosynthesis 63
RelA-dep. stringent response regulon (induced) 83
RelA-dep. stringent response regulon (repressed) 131
HrcA-dep. class I heat shock genes 9
CtsR-dep. class III heat shock genes 6
SigB-regulon (general stress response) 156
SigD-regulon (motility and chemotaxis genes) 63
SigH-regulon (stationary phase) 86
SigF-regulon (early sporulation genes) 22
SigE-regulon (early sporulation genes) 52
SigG-regulon (late sporulation genes) 38
SigK-regulon (late sporulation genes) 35
SigW-regulon (extracytoplasmic function) 60
SigM (extracytoplasmic function) 55
SigX (extracytoplasmic function) 32
minimum percentage
of induced genes
20%
40%
60%
of repressed genes
20%
40%
60%

indeed exhibited striking similarities in their expression profiles. The majority of genes induced or repressed by mupirocin and PTU belong to the *relA*-dependent stringent response network. This result is consistent with recent findings for the response of *B. subtilis* to norvaline, another AATS inhibitor (13). The most strongly induced gene cluster in our IleS-PheST inhibition and downregulation experiments was the *yur* cluster, including the putative operon *yurPONML* (Table 3). These genes are predicted to encode a sugar ABC transport system and sugar-metabolizing enzymes. Among the repressed genes, not only the stringently controlled genes could be found (especially the ones encoding the translation machinery), but also many genes involved in amino acid and nucleotide biosynthesis. Such a broad inhibition profile across different major biosynthetic pathways together with the stringent response could not be observed with antibiotics employing MOAs other than FAB and AATS. This explains the Wilcoxon classifier-based categorization of the FAB and AATS inhibitors into the same MOA category.

Remarkably, the transcriptional response to FAB inhibitors also exhibits similarities to the response caused by cell wall inhibitors, which is most strikingly visible when focusing on extracytoplasmic function (ECF) sigma factor regulons. ECF sigma factors regulate stress responses, typically triggered by changes in the cell envelope. For instance, vancomycin-caused stress to the cell envelope is known to induce the *sigW*- and *sigM*-dependent regulons and also *sigX*-dependent genes (11). In our experiments, such regulons were induced not only by vancomycin but also by beta-lactams such as oxacillin. And interestingly even the tested FAB inhibitors induced many genes regulated by those ECF sigma factors.

AATS target area analysis: target identification for compound PTU. While initially focusing on the global cellular responses, we then tried to utilize the large-scale expression data to identify the actual molecular target of a given antibiotic. For this purpose we also considered the 10-min data in addition to the 40-min compound treatment experiments, so that time-dependent changes in gene expression could be observed (Fig. 1B). Here, we wanted to exemplify this approach for the recently characterized MOA of PTU as a proof-of-concept case study.

Strikingly, the isoleucyl-tRNA synthetase inhibition by mupirocin led to induction of the target gene *ileS* (approximately four- to sixfold) but not of any other tRNA synthetase gene. On the other hand, PTU induced only *pheS* and *pheT* among all 26 tRNA synthetase genes (approximately twofold). No other antibiotic effect, including FAB inhibition, led to induction of any tRNA synthetase genes (exceptions: the threonyl-tRNA synthetase genes *thrZ* and *thrS*). In addition, the isoleucine-leucine biosynthesis genes were induced by mupirocin already after 10 min but not after 40 min (Fig. 1B). Consistent with these results, the *ileS* underexpression mutant showed slight induction of this amino acid biosynthesis pathway. Significantly fewer genes of this pathway were induced by PheST and FAB inhibition; the other tested antibiotics, independently of their underlying MOA, did not induce those genes at all. Correspondingly, the phenylalanine biosynthesis operon *pheAB* was slightly induced by PTU after 10 min (~1.6- to 1.9-fold) but not after 40 min of treatment. In summary, these results suggested that PheST is the molecular target of PTU. Indeed, PTU is a substance that has been identified in enzymatic high-throughput screening. By using complementary experimental approaches, only recently could it be independently shown that PTU kills bacteria by inhibition of PheST (5).

FAB target area analysis: target identification for MOIB. Next, we sought to identify the molecular target of the so-far-uncharacterized natural product MOIB. For this, we applied an approach similar to that used for PTU but also included a detailed pathway analysis. First, we mapped the mRNA expression fold factors onto the FAB-phospholipid biosynthesis pathway. This analysis revealed the sections of the pathway that were transcriptionally deregulated (Fig. 2). The *fabF* downregulation by a factor of 10 in mutant FABF(−) led to strong induction of *fabHB* (>10-fold; Table 3 and Fig. 2) and induction of *fabHA*, *plsC*, *fabD*, *fabG*, and *fabI* (>1.8-fold). All these genes are known to be transcriptionally controlled by the recently identified regulator FapR (16, 52). Exposure of *B. subtilis* to the FabF-targeting cerulenin also led to induction of these genes (Fig. 2). By contrast, the FapR-regulated genes are not induced by AATS inhibitors and other tested antibiotics (Fig. 1). They are partially repressed by non-FAB inhibitors such as, e.g., PTU, gentamicin, and chloramphenicol. Remarkably, MOIB represses all measurable FapR-regulated genes already after 10 min (Fig. 2). It is known that reduction of the cellular malonyl-CoA concentration leads to repression of FapR-regulated genes (52). The findings that the global transcriptional response of MOIB resembled more strongly a profile characteristic of FAB inhibitors than one of AATS inhibitors (Fig. 1A) and that the FapR-regulated genes were all repressed instead of being induced suggested that the *B. subtilis* malonyl-CoA pool might be reduced by this antibiotic. As

FIG. 1. Antibiotic-induced regulon and pathway activation pattern analysis of *B. subtilis*. The percentages of transcriptionally induced or repressed genes per biosynthetic pathway or regulon are represented in color codes (see color legend at the bottom of the figure). A deregulation of at least 20% of the genes of a pathway-regulon is required for a compound or underexpression effect to be indicated in the figure. Compound and mutant abbreviations can be found in Tables 2 and 3. The pathway and regulon assignments of the genes can be found online at http://www.genedata.com/publications/supplements/. For clarity, the most striking pathway activation patterns have been framed (black). (A) The compound-triggered mRNA profiles all represent long-time exposure experiments (*t*, 40-min treatments). The compounds and mutants are sorted according to their MOA categories as known from the literature and as concluded from our transcriptome studies (abbreviations for MOA classes are in Table 5). (B) Time-dependent antibiotic-induced regulon and pathway activation pattern analysis of *B. subtilis*. The numbers after the compound abbreviations symbolize compound treatment times (1 = 10 min; 2 = 40 min). The compounds and mutants are sorted according to their target area assignment (see text). # indicates that, while a significant proportion of the aromatic biosynthesis genes are repressed under condition PTU1 (10-min treatment with the PheST inhibitor), the phenylalanine biosynthesis operon *pheAB* is slightly induced, which is not the case in any other measured stress condition.

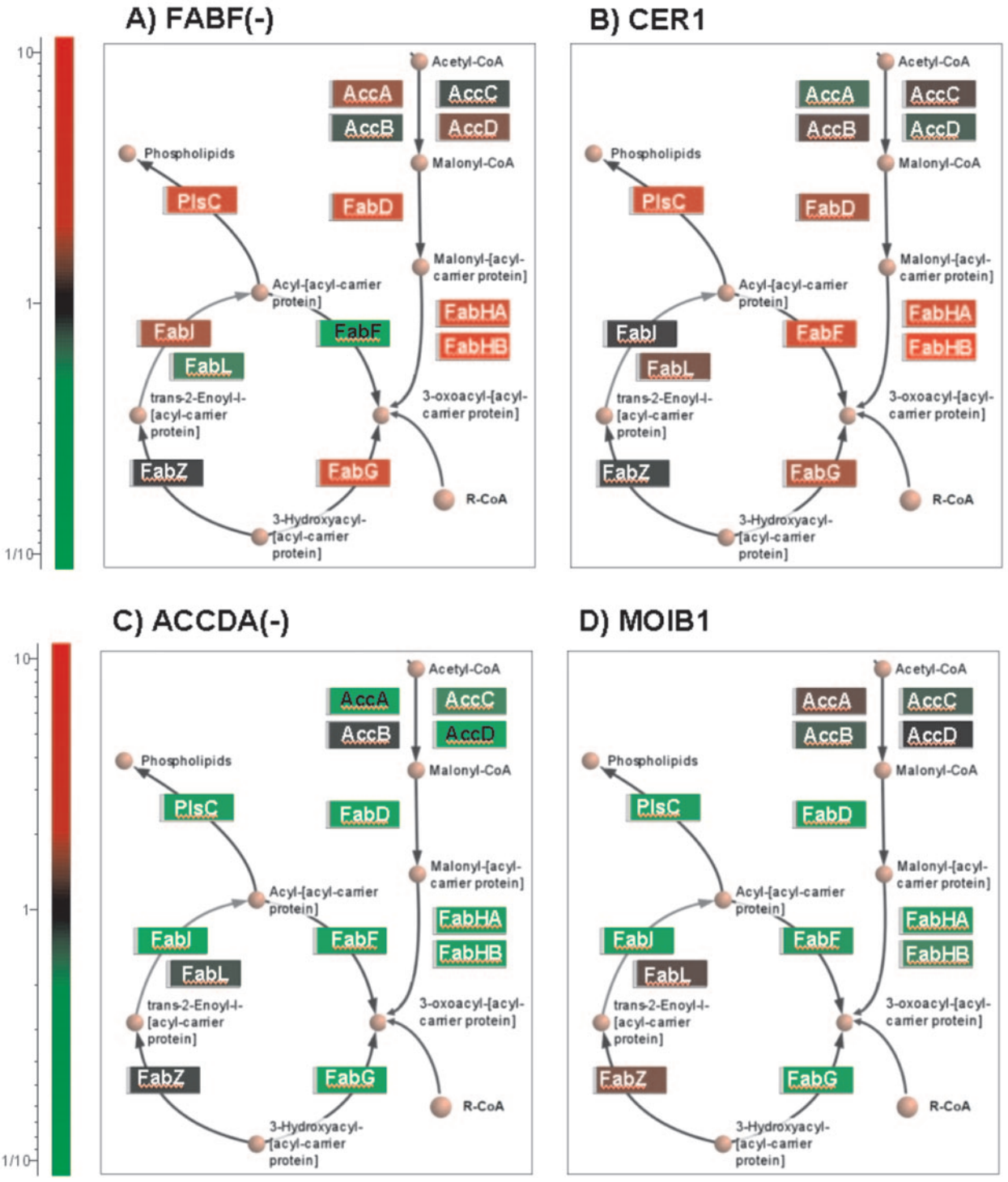

FIG. 2. Transcriptional activation pattern of the *B. subtilis* fatty acid and phospholipid biosynthesis pathway for antibiotic treatment and the modified gene expression due to target underexpression. (A) Mutant with downregulated *fabF*; (B) treatment of *B. subtilis* 168 with cerulenin for 10 min; (C) mutant with downregulated *accDA*; (D) treatment of *B. subtilis* 168 with MOIB for 10 min (Phylosopher; Genedata). FabF repression and cerulenin treatment mainly induce genes encoding enzymes downstream of the metabolite malonyl-CoA. In contrast to this finding, treatment with MOIB and *accDA* repression mainly repress those genes. This pathway analysis indicated that cerulenin targets FabF, while MOIB possibly inhibits the ACC. Upregulated genes are colored in red, while downregulated genes are represented by green boxes; see color scale at left. Nonresponsive genes are colored in gray (metabolite names: R, acetyl, isovaleryl, 2-methylbuturyl, or isobutyryl).

the key enzyme responsible for malonyl-CoA synthesis is the ACC, we hypothesized that ACC inhibition might be the reason for the observed characteristic mRNA profiles.

To test this hypothesis, we generated a xylose-dependent ACCDA(−) mutant, which indeed showed differential sensitivity towards MOIB (Table 4). When measuring the transcriptional response to ~10-fold downregulation of these two carboxyltransferase subunits of ACC, all FapR-dependent genes were strongly repressed (Fig. 2), as in the case of the MOIB treatment experiments. This reasoning suggested that MOIB represents an antibacterial agent acting via inhibition of ACC. In the meantime, the ACC has been independently confirmed to be the target of MOIB, by using complementary experimental techniques (17).

DISCUSSION

Global genomics technologies such as proteome and transcriptome analyses represent novel tools to characterize the MOA of antibacterial agents. Here, we used *B. subtilis*, a gram-positive bacterium which is a favored model organism in this respect because of advanced physiological knowledge and its phylogenetic relationship to major pathogens such as staphylococci, enterococci, and streptococci. Recently, a proteomic study with antibiotics has been published, followed by a transcriptome study (3, 30). While the proteome study focused on a limited number of gene products to discriminate antibiotic MOAs, the transcriptome study took into account the expression activity of virtually all ~4,100 *B. subtilis* genes. Thus, the large data volumes generated by microarray technologies require systematic data analysis techniques to characterize the MOA of antibiotics. Previously, it was shown that simple expression clustering or standard correlation analyses performed only poorly for compound MOA analyses (6, 23, 30, 50, 57). More appropriate algorithms that have been suggested for MOA classification purposes are support vector machines, k-nearest neighbor analysis, sparse linear discriminant analysis, and Fisher linear discriminant analysis (65). The results presented here are based on the Wilcoxon classifier, as implemented in the Expressionist system (Genedata). A cross-validation analysis showed that this classifier worked very well with the data produced in this study. A comparison with predictions based on other classification methods gave an overall consistent picture (data to be published elsewhere).

The application of classification tools is the first step in the interpretation of complex transcriptome data in drug discovery. As each expression value is coupled to individual genes embedded in known functional and regulatory networks, the data can be alternatively interpreted from the physiological point of view. Therefore, we also investigated the transcriptional activity of the major regulatory units and biosynthetic pathways of *B. subtilis*. This helped to biologically interpret the computer-based MOA classification results. For instance, the stringent response regulon represents a global regulatory unit whose deregulation was indicative of AATS as well as FAB inhibition, leading to the classification of FAB and AATS inhibitors into one category (55).

In this study, we investigated the value of conditional mutants for the detection of completely novel MOAs. Applying classification algorithms together with regulon and pathway analyses, we were able to show that the directed downregulation of genes indeed led to transcriptional responses being equivalent to chemical inhibition of the corresponding gene products. We demonstrated this by measuring the mRNA profiles of mutants whose target genes were downregulated by xylose depletion. For instance, the FABF(−) mutant showed an induction of the genes regulated by the fatty acid-phospholipid biosynthesis regulator FapR, while *accDA* downregulation led to repression of those genes. The *ileS* underexpression led to an induction of isoleucine biosynthesis genes, which is consistent with the view that the cells sense starvation of amino acid biosynthesis in the case of inhibition of the respective AATS. Only the PHEST(−) mutant did not reveal deregulation of genes directly linked to the repressed target operon. One reason for this observation might be the very strong repression of the *pheST* operon (~50-fold), which already led to a strong global stress response including activation of sporulation genes (Fig. 1B). In addition, all four mutants showed secondary responses equivalent to the effects of the respective antibiotics, including the stringent response as well as induction of *sigM-sigX*-dependent genes in the case of *fabF* and *accDA* downregulation.

Briefly put, the primary effects affecting the target area and the broad secondary responses appear to be superposed in the expression profiles of the underexpression mutants. In contrast, the antibiotic treatment experiments revealed that the primary effects on the target area were often seen already after 10 min but were no longer detectable after 40 min (e.g., for PTU and MOIB), while the global secondary responses were more pronounced after 40 min. However, the data analysis techniques used in this work were still able to detect the underlying MOAs of the compounds, as was demonstrated by classifying the late-stage stress response profiles. The difference between the continuous underexpression of essential target genes and the inhibition of cell growth by antibiotic treatment for a defined time frame might explain the observed concurrence or chronology of primary and secondary responses. Nevertheless, we could show that the global characteristics of underexpression mutant profiles are equivalent to antibiotic treatment profiles, enabling the classification of antibiotics employing novel MOAs, as was shown for PTU and MOIB.

Comprehensive cross-validation studies showed that automated MOA classification of the 40-min mRNA profiles consistently resulted in superior classification rates compared to the cross-validation of the 10-min mRNA profiles (data not shown). Apparently, the higher number of deregulated genes after 40 min than at the earlier time points provides a more reliable basis for MOA classification purposes. In fact, the global MOA classification approach was an essential prerequisite to identify, for instance, the FAB pathway as the primary target area of MOIB. Once the broad target area had been pinpointed, early time point experiments were essential for studying the primary antibiotic effects and predicting the molecular targets such as ACC in the case of MOIB.

Transcriptome analyses as well as differential sensitivity tests with underexpression systems always represent indirect methods to prove inhibition effects of antibiotics. Therefore, it is difficult to decide whether other gene products, the expression of which is strictly coupled to the predicted target (here, e.g.,

accDA), might be the actual molecular target of the investigated antibiotic (here, e.g., MOIB). In the context of MOIB, it is worthwhile to mention that underexpression of the *accBC* operon leads to repression of the two FapR-dependent operons *fabHAF* and *fabHB* (52). The AccBC subunits complete the ACC complex, consisting of the carboxyltransferase subunits AccDA, the biotin carboxylase AccC, and the biotin-carboxyl carrier protein AccB. We therefore cannot discriminate which part of the ACC complex might be targeted by MOIB. In addition, blockage of the biotin synthesis or biotinylation of ACC might cause effects on the transcriptome similar to the ones caused by *accDA* downregulation. Although this issue has not been addressed in this study, it would be straightforward to apply our proposed analysis strategy to conditional mutants regulating the upstream biotin pathway. Nevertheless, our reference compendium approach together with the differential sensitivity test with the ACCDA(−) mutant gave consistent results, which narrow down the target area of MOIB to the start of the FAB pathway, with ACC as the most likely target candidate. To our knowledge, no antibiotic that targets ACC has been described yet. This means that our suggested approach with an extended mutant reference compendium can indeed be used to predict novel mechanisms of antibiotics, as demonstrated by MOIB's ACC inhibition.

In conclusion, we show that a combined statistical data analysis of a compendium of diverse global mRNA profiles, together with a thorough pathway and regulon analysis, can pinpoint the molecular target of antibiotics. We systematically analyzed the transcriptional activity of 28 major *B. subtilis* regulons and groups of biosynthetic pathways. Consideration of more regulatory units will most likely improve the MOA prediction accuracy and further our understanding of the response of bacteria to antibiotic stress. Obviously, addressing novel MOAs is very important, as many promising target areas are not exploited by the currently available antibiotics and can therefore not be used for a reference compendium approach. Thus, the inclusion of conditional mutants in antibiotic-based reference compendia significantly widens existing opportunities for these technologies. We were able to show that, whenever reference antibiotics are not available, conditional mutants can be used to mimic chemical inhibition of the corresponding gene products. The confirmation of the MOA of PTU as a PheST inhibitor and the prediction of the ACC as the target of MOIB validate the usefulness of such mutants for MOA predictions of uncharacterized bioactive compounds.

ACKNOWLEDGMENTS

We thank U. Reimann and M. Haas for technical assistance. We are grateful to T. Freeman for critically reading the manuscript.

REFERENCES

1. **Amaya, E., A. Khvorova, and P. J. Piggot.** 2001. Analysis of promoter recognition in vivo directed by σ^F of *Bacillus subtilis* by using random-sequence oligonucleotides. J. Bacteriol. **183:**3623–3630.
2. **Asai, K., H. Yamaguchi, C. M. Kang, K. Yoshida, Y. Fujita, and Y. Sadaie.** 2003. DNA microarray analysis of *Bacillus subtilis* sigma factors of extracytoplasmic function family. FEMS Microbiol. Lett. **220:**155–160.
3. **Bandow, J. E., H. Brotz, L. I. Leichert, H. Labischinski, and M. Hecker.** 2003. Proteomic approach to understanding antibiotic action. Antimicrob. Agents Chemother. **47:**948–955.
4. **Betts, J. C., A. McLaren, M. G. Lennon, F. M. Kelly, P. T. Lukey, S. J. Blakemore, and K. Duncan.** 2003. Signature gene expression profiles discriminate between isoniazid-, thiolactomycin-, and triclosan-treated *Mycobacterium tuberculosis*. Antimicrob. Agents Chemother. **47:**2903–2913.
5. **Beyer, D., H. P. Kroll, R. Endermann, G. Schiffer, S. Siegel, M. Bauser, J. Pohlmann, M. Brands, K. Ziegelbauer, D. Haebich, C. Eymann, and H. Brötz-Oesterhelt.** 2004. New class of bacterial phenylalanyl-tRNA synthetase inhibitors with high potency and broad-spectrum activity. Antimicrob. Agents Chemother. **48:**525–532.
6. **Bhattacharjee, A., W. G. Richards, J. Staunton, C. Li, S. Monti, P. Vasa, C. Ladd, J. Beheshti, R. Bueno, M. Gillette, M. Loda, G. Weber, E. J. Mark, E. S. Lander, W. Wong, B. E. Johnson, T. R. Golub, D. J. Sugarbaker, and M. Meyerson.** 2001. Classification of human lung carcinomas by mRNA expression profiling reveals distinct adenocarcinoma subclasses. Proc. Natl. Acad. Sci. USA **98:**13790–13795.
7. **Breithaupt, H.** 1999. The new antibiotics. Nat. Biotechnol. **17:**1165–1169.
8. **Britton, R. A., P. Eichenberger, J. E. Gonzalez-Pastor, P. Fawcett, R. Monson, R. Losick, and A. D. Grossman.** 2002. Genome-wide analysis of the stationary-phase sigma factor (sigma-H) regulon of *Bacillus subtilis*. J. Bacteriol. **184:**4881–4890.
9. **Cao, M., and J. D. Helmann.** 2002. Regulation of the *Bacillus subtilis bcrC* bacitracin resistance gene by two extracytoplasmic function sigma factors. J. Bacteriol. **184:**6123–6129.
10. **Cao, M., P. A. Kobel, M. M. Morshedi, M. F. Wu, C. Paddon, and J. D. Helmann.** 2002. Defining the *Bacillus subtilis* σ^W regulon: a comparative analysis of promoter consensus search, run-off transcription/macroarray analysis (ROMA), and transcriptional profiling approaches. J. Mol. Biol. **316:**443–457.
11. **Cao, M., T. Wang, R. Ye, and J. D. Helmann.** 2002. Antibiotics that inhibit cell wall biosynthesis induce expression of the *Bacillus subtilis* σ^W and σ^M regulons. Mol. Microbiol. **45:**1267–1276.
12. **Chopra, I., L. Hesse, and A. J. O'Neill.** 2002. Exploiting current understanding of antibiotic action for discovery of new drugs. J. Appl. Microbiol. **92**(Suppl.)**:**4S–15S.
13. **Eymann, C., G. Homuth, C. Scharf, and M. Hecker.** 2002. *Bacillus subtilis* functional genomics: global characterization of the stringent response by proteome and transcriptome analysis. J. Bacteriol. **184:**2500–2520.
14. **Fawcett, P., P. Eichenberger, R. Losick, and P. Youngman.** 2000. The transcriptional profile of early to middle sporulation in *Bacillus subtilis*. Proc. Natl. Acad. Sci. USA **97:**8063–8068.
15. **Ferrari, F. A., A. Nguyen, D. Lang, and J. A. Hoch.** 1983. Construction and properties of an integrable plasmid for *Bacillus subtilis*. J. Bacteriol. **154:** 1513–1515.
16. **Fischer, H. P., N. A. Brunner, B. Wieland, J. Paquette, L. Macko, K. Ziegelbauer, and C. Freiberg.** 2004. Identification of antibiotic stress-inducible promoters: a systematic approach to novel pathway-specific reporter assays for antibacterial drug discovery. Genome Res. **14:**90–98.
17. **Freiberg, C., G. Schiffer, N. Brunner, T. Lampe, J. Pohlmann, M. Brands, D. Haebich, and K. Ziegelbauer.** 2004. Identification and characterization of the first class of potent bacterial acetyl-CoA carboxylase inhibitors with antibacterial activity. J. Biol. Chem. **279:**26066–26073.
18. **Fujita, M.** 1999. Identification of new sigma K-dependent promoters using an in vitro transcription system derived from *Bacillus subtilis*. Gene **237:**45–52.
19. **Gmuender, H., K. Kuratli, K. Di Padova, C. P. Gray, W. Keck, and S. Evers.** 2001. Gene expression changes triggered by exposure of *Haemophilus influenzae* to novobiocin or ciprofloxacin: combined transcription and translation analysis. Genome Res. **11:**28–42.
20. **Goh, E. B., G. Yim, W. Tsui, J. McClure, M. G. Surette, and J. Davies.** 2002. Transcriptional modulation of bacterial gene expression by subinhibitory concentrations of antibiotics. Proc. Natl. Acad. Sci. USA **99:**17025–17030.
21. **Guedon, E., C. M. Moore, Q. Que, T. Wang, R. W. Ye, and J. D. Helmann.** 2003. The global transcriptional response of *Bacillus subtilis* to manganese involves the MntR, Fur, TnrA and σB regulons. Mol. Microbiol. **49:**1477–1491.
22. **Guerout-Fleury, A. M., N. Frandsen, and P. Stragier.** 1996. Plasmids for ectopic integration in *Bacillus subtilis*. Gene **180:**57–61.
23. **Gunther, E. C., D. J. Stone, R. W. Gerwien, P. Bento, M. P. Heyes, J. E. Staunton, D. K. Slonim, H. A. Coller, P. Tamayo, M. J. Angelo, J. Park, U. Scherf, J. K. Lee, W. O. Reinhold, J. N. Weinstein, J. P. Mesirov, E. S. Lander, T. R. Golub, A. Bhattacharjee, W. G. Richards, J. Staunton, C. Li, S. Monti, P. Vasa, C. Ladd, J. Beheshti, R. Bueno, M. Gillette, M. Loda, G. Weber, E. J. Mark, W. Wong, B. E. Johnson, D. J. Sugarbaker, and M. Meyerson.** 2003. Prediction of clinical drug efficacy by classification of drug-induced genomic expression profiles in vitro. Proc. Natl. Acad. Sci. USA **100:**9608–9613.
24. **Haas, M., D. Beyer, R. Gahlmann, and C. Freiberg.** 2001. YkrB is the main peptide deformylase in *Bacillus subtilis*, a eubacterium containing two functional peptide deformylases. Microbiology **147:**1783–1791.
25. **Haldenwang, W. G.** 1995. The sigma factors of *Bacillus subtilis*. Microbiol. Rev. **59:**1–30.
26. **Harwood, C. R., and S. M. Cutting.** 1990. Molecular biological methods for *Bacillus*. Wiley, Chichester, United Kingdom.
27. **Horsburgh, M. J., and A. Moir.** 1999. Sigma M, an ECF RNA polymerase sigma factor of *Bacillus subtilis* 168, is essential for growth and survival in high concentrations of salt. Mol. Microbiol. **32:**41–50.

28. **Huang, X., and J. D. Helmann.** 1998. Identification of target promoters for the *Bacillus subtilis* sigma X factor using a consensus-directed search. J. Mol. Biol. **279:**165–173.
29. **Hughes, J., and G. Mellows.** 1980. Interaction of pseudomonic acid A with *Escherichia coli* B isoleucyl-tRNA synthetase. Biochem. J. **191:**209–219.
30. **Hutter, B., C. Schaab, S. Albrecht, M. Borgmann, N. A. Brunner, C. Freiberg, K. Ziegelbauer, C. O. Rock, I. Ivanov, and H. Loferer.** 2004. Prediction of mechanisms of action of antibacterial compounds by gene expression profiling. Antimicrob. Agents Chemother. **48:**2838–2844.
31. **Ishii, T., K. Yoshida, G. Terai, Y. Fujita, and K. Nakai.** 2001. DBTBS: a database of *Bacillus subtilis* promoters and transcription factors. Nucleic Acids Res. **29:**278–280.
32. **Ishikawa, S., K. Yamane, and J. Sekiguchi.** 1998. Regulation and characterization of a newly deduced cell wall hydrolase gene (*cwlJ*) which affects germination of *Bacillus subtilis* spores. J. Bacteriol. **180:**1375–1380.
33. **Itaya, M., K. Kondo, and T. Tanaka.** 1989. A neomycin resistance gene cassette selectable in a single copy state in the *Bacillus subtilis* chromosome. Nucleic Acids Res. **17:**4410.
34. **Kauppinen, S., M. Siggaard-Andersen, and P. von Wettstein-Knowles.** 1988. β-Ketoacyl-ACP synthase I of *Escherichia coli*: nucleotide sequence of the *fabB* gene and identification of the cerulenin binding residue. Carlsberg Res. Commun. **53:**357–370.
35. **Kodama, T., H. Takamatsu, K. Asai, K. Kobayashi, N. Ogasawara, and K. Watabe.** 1999. The *Bacillus subtilis yaaH* gene is transcribed by SigE RNA polymerase during sporulation, and its product is involved in germination of spores. J. Bacteriol. **181:**4584–4591.
36. **Kubitschek, H. E., and R. J. Sepanski.** 1982. Azaserine: survival and mutation in *Escherichia coli*. Mutat. Res. **94:**31–38.
37. **Lawson, T.** 1989. Nicotinamide and selenium stimulate the repair of DNA damage produced by *N*-nitrosobis (2-oxopropyl) amine. Anticancer Res. **9:**483–486.
38. **Mascher, T., N. G. Margulis, T. Wang, R. W. Ye, and J. D. Helmann.** 2003. Cell wall stress responses in *Bacillus subtilis*: the regulatory network of the bacitracin stimulon. Mol. Microbiol. **50:**1591–1604.
39. **Mirel, D. B., W. F. Estacio, M. Mathieu, E. Olmsted, J. Ramirez, and L. M. Marquez-Magana.** 2000. Environmental regulation of *Bacillus subtilis* σ^D-dependent gene expression. J. Bacteriol. **182:**3055–3062.
40. **Moche, M., G. Schneider, P. Edwards, K. Dehesh, and Y. Lindqvist.** 1999. Structure of the complex between the antibiotic cerulenin and its target, beta-ketoacyl-acyl carrier protein synthase. J. Biol. Chem. **274:**6031–6034.
41. **Mwangi, M. M., and E. D. Siggia.** 2003. Genome wide identification of regulatory motifs in *Bacillus subtilis*. BMC Bioinformatics **4:**18.
42. **Needham, J., M. T. Kelly, M. Ishige, and R. J. Andersen.** 1994. Andrimid and moiramides A-C, metabolites produced in culture by a marine isolate of the bacterium *Pseudomonas fluorescens*: structure elucidation and biosynthesis. J. Org. Chem. **59:**2058–2063.
43. **Ng, W. L., K. M. Kazmierczak, G. T. Robertson, R. Gilmour, and M. E. Winkler.** 2003. Transcriptional regulation and signature patterns revealed by microarray analyses of *Streptococcus pneumoniae* R6 challenged with sublethal concentrations of translation inhibitors. J. Bacteriol. **185:**359–370.
44. **Nugroho, F. A., H. Yamamoto, Y. Kobayashi, and J. Sekiguchi.** 1999. Characterization of a new sigma-K-dependent peptidoglycan hydrolase gene that plays a role in *Bacillus subtilis* mother cell lysis. J. Bacteriol. **181:**6230–6237.
45. **Perego, M., and J. A. Hoch.** 2001. Functional genomics of gram-positive microorganisms: review of the meeting, San Diego, California, 24 to 28 June 2001. J. Bacteriol. **183:**6973–6978.
46. **Petersohn, A., M. Brigulla, S. Haas, J. D. Hoheisel, U. Volker, and M. Hecker.** 2001. Global analysis of the general stress response of *Bacillus subtilis*. J. Bacteriol. **183:**5617–5631.
47. **Price, C. W., P. Fawcett, H. Ceremonie, N. Su, C. K. Murphy, and P. Youngman.** 2001. Genome-wide analysis of the general stress response in *Bacillus subtilis*. Mol. Microbiol. **41:**757–774.
48. **Qiu, J., and J. D. Helmann.** 2001. The −10 region is a key promoter specificity determinant for the *Bacillus subtilis* extracytoplasmic-function sigma factors σ^X and σ^W. J. Bacteriol. **183:**1921–1927.
49. **Ragkousi, K., P. Eichenberger, C. van Ooij, and P. Setlow.** 2003. Identification of a new gene essential for germination of *Bacillus subtilis* spores with Ca^{2+}-dipicolinate. J. Bacteriol. **185:**2315–2329.
50. **Ramaswamy, S., P. Tamayo, R. Rifkin, S. Mukherjee, C. H. Yeang, M. Angelo, C. Ladd, M. Reich, E. Latulippe, J. P. Mesirov, T. Poggio, W. Gerald, M. Loda, E. S. Lander, and T. R. Golub.** 2001. Multiclass cancer diagnosis using tumor gene expression signatures. Proc. Natl. Acad. Sci. USA **98:**15149–15154.
51. **Sabina, J., N. Dover, L. J. Templeton, D. R. Smulski, D. Soll, and R. A. LaRossa.** 2003. Interfering with different steps of protein synthesis explored by transcriptional profiling of *Escherichia coli* K-12. J. Bacteriol. **185:**6158–6170.
52. **Schujman, G. E., L. Paoletti, A. D. Grossman, and D. de Mendoza.** 2003. FapR, a bacterial transcription factor involved in global regulation of membrane lipid biosynthesis. Dev. Cell **4:**663–672.
53. **Schumann, W.** 2003. The *Bacillus subtilis* heat shock stimulon. Cell Stress Chaperones **8:**207–217.
54. **Serrano, M., S. Hovel, C. P. Moran, Jr., A. O. Henriques, and U. Volker.** 2001. Forespore-specific transcription of the *lonB* gene during sporulation in *Bacillus subtilis*. J. Bacteriol. **183:**2995–3003.
55. **Seyfzadeh, M., J. Keener, and M. Nomura.** 1993. *spoT*-dependent accumulation of guanosine tetraphosphate in response to fatty acid starvation in *Escherichia coli*. Proc. Natl. Acad. Sci. USA **90:**11004–11008.
56. **Shaw, K. J., N. Miller, X. Liu, D. Lerner, J. Wan, A. Bittner, and B. J. Morrow.** 2003. Comparison of the changes in global gene expression of *Escherichia coli* induced by four bactericidal agents. J. Mol. Microbiol. Biotechnol. **5:**105–122.
57. **Staunton, J. E., D. K. Slonim, H. A. Coller, P. Tamayo, M. J. Angelo, J. Park, U. Scherf, J. K. Lee, W. O. Reinhold, J. N. Weinstein, J. P. Mesirov, E. S. Lander, T. R. Golub, A. Bhattacharjee, W. G. Richards, J. Staunton, C. Li, S. Monti, P. Vasa, C. Ladd, J. Beheshti, R. Bueno, M. Gillette, M. Loda, G. Weber, E. J. Mark, W. Wong, B. E. Johnson, D. J. Sugarbaker, and M. Meyerson.** 2001. Chemosensitivity prediction by transcriptional profiling. Proc. Natl. Acad. Sci. USA **98:**10787–10792.
58. **Stulke, J., R. Hanschke, and M. Hecker.** 1993. Temporal activation of beta-glucanase synthesis in *Bacillus subtilis* is mediated by the GTP pool. J. Gen. Microbiol. **139:**2041–2045.
59. **Takamatsu, H., T. Kodama, T. Nakayama, and K. Watabe.** 1999. Characterization of the *yrbA* gene of *Bacillus subtilis*, involved in resistance and germination of spores. J. Bacteriol. **181:**4986–4994.
60. **Tatusov, R. L., N. D. Fedorova, J. J. Jackson, A. R. Jacobs, B. Kiryutin, E. V. Koonin, D. M. Krylov, R. Mazumder, S. L. Mekhedov, A. N. Nikolskaya, B. S. Rao, S. Smirnov, A. V. Sverdlov, S. Vasudevan, Y. I. Wolf, J. J. Yin, and D. A. Natale.** 2003. The COG database: an updated version includes eukaryotes. BMC Bioinformatics **4:**41.
61. **Thackray, P. D., and A. Moir.** 2003. SigM, an extracytoplasmic function sigma factor of *Bacillus subtilis*, is activated in response to cell wall antibiotics, ethanol, heat, acid, and superoxide stress. J. Bacteriol. **185:**3491–3498.
62. **Wiegert, T., G. Homuth, S. Versteeg, and W. Schumann.** 2001. Alkaline shock induces the *Bacillus subtilis* σ^W regulon. Mol. Microbiol. **41:**59–71.
63. **Wilson, M., J. DeRisi, H. H. Kristensen, P. Imboden, S. Rane, P. O. Brown, and G. K. Schoolnik.** 1999. Exploring drug-induced alterations in gene expression in *Mycobacterium tuberculosis* by microarray hybridization. Proc. Natl. Acad. Sci. USA **96:**12833–12838.
64. **Yamamoto, H., M. Mori, and J. Sekiguchi.** 1999. Transcription of genes near the *sspE* locus of the *Bacillus subtilis* genome. Microbiology **145:**2171–2180.
65. **Yeang, C. H., S. Ramaswamy, P. Tamayo, S. Mukherjee, R. M. Rifkin, M. Angelo, M. Reich, E. Lander, J. Mesirov, and T. Golub.** 2001. Molecular classification of multiple tumor types. Bioinformatics **17**(Suppl. 1)**:**S316–S322.